


DETERMINATION OF THE AGMA J-FACTOR FOR INTERNAL SPUR GEARS

A close-up photograph of a gear tooth root fillet, showing the intricate geometry and the smooth transition between the tooth and the root. The image is in a blue-tinted, high-contrast style, highlighting the texture and curvature of the metal surface.

The AGMA J -factor is calculated in four different ways by considering the maximum total stress and minimum curvature radius of the trochoid fillet, the maximum total stress and curvature radius at the corresponding tooth section, the maximum total stress and circular fillet, and the maximum total stress obtained from FEM analyses.

By ALFONSO FUENTES-AZNAR and JOSÉ I. PEDRERO

The Geometry Factor for Bending Strength, J , also known as AGMA J -factor, is used to assess the tooth-root stress of spur and helical gear teeth. The Information Sheet AGMA 908-B89 presents a calculation method for the AGMA J -factor based on the Lewis' parabola and computes the stress concentration factor from the minimum curvature radius of the fillet trochoid. Although the presented basic gear geometry is valid for external and internal gears, it was stated that the method for the analytical determination of the AGMA J -factor was not appropriate for internal gears, and it was beyond the scope of the Standard.

By using the Lewis' method, the tooth section with maximum bending stress is calculated and the tooth-root stress determined. However, the modern definition of tooth-root stress considers other influences than pure bending, and, therefore, the Information Sheet AGMA 911-B21 suggests considering the highest total stress, including the compressive stress and the stress concentration at the considered section. In addition, the root-fillet trochoid is approximated to a circumference arc, and the influence of the number of teeth and shift coefficient of the shaper is neglected.

In this article, the AGMA J -factor is calculated in four different ways by considering: (i) the maximum total stress and minimum curvature radius of the trochoid fillet, (ii) the maximum total stress and curvature radius at the corresponding tooth section, (iii) the maximum total stress and circular fillet, and (iv) the maximum total stress obtained from FEM analyses. Based on the comparison of the results of the mentioned four approaches, guidelines for the preparation of a proposal for the calculation of the AGMA J -factor for internal gears are provided. It has been demonstrated that, for internal gears generated by a shaper, the number of teeth and the profile shift coefficient of the shaper influences the values of the J -factor.

1 INTRODUCTION

In order to ensure gears are capable of supporting the loads and stresses they experience during their operation due to the transmitted power, gear designers must carefully consider the tooth root stresses in the process of gear design. Fatigue failure by tooth root

stresses is considered a catastrophic failure that should be avoided because it permanently damages the gears and compromises the safety of the system in which the gears are used.

The first model to determine the bending stress on gear teeth was based on the Lewis form factor, Y . The Lewis form factor, Y , was developed by Wilfred Lewis in 1893 [1]. It was widely used in the industry for many years and served as a useful tool for gear design. However, it had some limitations, such as not considering the compression due to the radial component of the normal force or not considering the stress concentration at the root trochoid.

The first known investigation of stress concentration at the root profile of gear teeth was performed by Dolan and Broghamer in 1942 [2] by using a photoelastic method. It was done for external gears, and it is still applied today. However, its application to internal gears is yet to be assessed.

About 1960, the American Gear Manufacturers Association (AGMA) presented a method for calculating the gear tooth bending stress, based on the so-called AGMA J -factor. The J -factor method improves upon the limitations of the Lewis form factor by taking into account the stress concentration at the root fillet, the geometry of the fillet, and the operating conditions throughout the location of the point of application of the load. At the beginning, the J -factor was calculated by graphical methods, which obviously provided very low-precision results. It was Errichello in 1983 [3] who developed the algorithm for the J -factor for external spur and helical gears generated by pinion-type shaper cutters. This algorithm was adopted by AGMA as the official method for calculating the J -factor and was included in the computational method presented in AGMA 908-B89 [4].

Mitchiner and Mabie [5] presented a simple and direct approach to the problem of definition of the root profile for standard and nonstandard external spur gear teeth. They developed the equations to determine the location of the point of tangency of a constant-stress parabola with the root trochoid, in which the critical section of the gear tooth is established to get the J -factor.

Carroll and Johnson [6] presented an approximate equation for the J -factor, which could be useful for computer applications and avoided the convergency problems of the iterative procedures. However, it was only valid for rack-generated spur gears with no backlash, no tool shift, and standard center distance, which results in a very narrow scope. Pedrero et al. [7] presented an approximate method for the determination of the critical section parameters (location, thickness, and curvature radius), from which the J -factor can be computed analytically, which is valid for any set of tooth proportions, tooth numbers, shift coefficients, operating center distances, helix angles, and contact ratios. Arikan [8,9] developed analytical expressions for the J -factor for external spur gears by using polynomial equations, which can be used to calculate the tooth root stresses corresponding to loads acting on any point on the involute tooth profile.

However, there is not much investigation of the AGMA J -factor for internal spur and helical gears. The available information refers to AGMA 911-B21 [10] that, in its Annex A, provides a method to determine the J -factor for internal gears, but it is intended for informative purposes only. No standard has been established yet for the determination of the J -factor for internal spur and helical gears.

Some of the assumptions in the method presented in the informational Annex A of AGMA 911-B21 include:

- 1: The fillet geometry corresponds to a true ground fillet, which is a circular arc, and, therefore, the actual geometry of the trochoid generated by the tip edge of the generating shaper is not being considered.
- 2: The number of teeth of the shaper is not considered at all.
- 3: The radial component of the normal force is being considered and, therefore, the maximum tensile bending stress at the tooth fillet will be reduced by the compressive stress caused by the radial force.
- 4: A stress concentration factor, which is a function of the dimensions and location of the critical section, is used based on a modified version of the stress concentration factor proposed by Dolan and Broghamer [2].

5: The critical section is determined by an iterative method to find the section in which the total stress, considering tension due to the bending moment, and compression due to the radial force is maximum and not where the highest bending stress is maximum.

This article is intended to advance in establishing an accurate procedure for the determination of the J -factor in internal gears and determine some important dependencies that may not have been considered yet. An effort has also been made to show the values of the J -factor that would be obtained by using the maximum principal stresses at the fillet of the gear teeth by the Finite Element Method (FEM). It will establish how far the actual methodology is from predicting the tooth root stresses at the internal gear root fillets as obtained by the FE method.

2 THE AGMA J -FACTOR

According to the model in which the calculation methods outlined in ANSI/AGMA 2001-D04 [11] are based on, the relation between the critical stress at the tooth-root of a spur gear, denoted as σ_b , and the AGMA J -factor, can be expressed as follows:

$$\sigma_b = \frac{W_t}{J F m_n} \quad \text{Equation 2.1}$$

where:

- W_t is the tangential load at the operating pitch radius.
 - F is the face width.
 - m_n is the normal module.
 - J is the geometry factor for bending strength (AGMA J -factor).
- The combination of Equation 2.1 and the equations of the linear

theory of elasticity results in a J -factor to be calculated as follows:

$$J = \frac{1}{m_n K_f} \frac{1}{\cos \phi_{nL} \left(\frac{6h_F}{S_F^2} - \frac{\tan \phi_{nL}}{S_F} \right)} \quad \text{Equation 2.2}$$

where:

- K_f is the stress correction factor.
- ϕ_{nL} is the load angle at the highest point of single tooth contact (HPSTC).
- ϕ_{nr} is the operating normal pressure angle.
- h_F is the moment arm.
- S_F is the tooth thickness at the critical tooth section.

Equations 2.1 and 2.2 are suitable for assessing the stress at any section of the tooth root and any load point, but for strength calculations, the critical load point and critical section in which the stress is maximum should be determined. In this article, the J -factor will be assessed first from three analytical approaches consisting of different assumptions on the location of the critical section and the stress correction factor. The critical load condition always corresponds to the total load acting at the HPSTC of the corresponding gear.

3 ANALYTICAL APPROACHES

In this article, the following three analytical approaches will be considered:

- Approach #1, based on AGMA 908-B89 [4].
- Approach #2, based on AGMA 911-B21 [10], Annex A.
- Approach #3, based on a hybrid model combining the previous two models. All of them are briefly described in the following subsections.

3.1 APPROACH #1, BASED ON AGMA 908-B89

For external gears, AGMA 908-B89 [4] provides a calculation method of the J -factor based on the following assumptions:

- Both the bending component and the compressive component of the stress at the root should be considered.
- Stresses should be calculated at the tooth-root section defined by the tangency point of the Lewis parabola and the tooth-root trochoid, for the load acting at the HPSTC.

► The stress correction factor should be considered according to the Dolan and Broghamer Equation 2. Accordingly, the curvature radius of the root fillet to be considered should be the minimum curvature radius of the trochoid, and, therefore, the one corresponding to the intersection point of the fillet trochoid and the root circle.

To apply this model to the calculation of the J -factor of internal gears, the equations of the tooth thickness at the root, the moment arm, the curvature radius of the root trochoid and the load angle should be obtained.

The parametric polar equations (r , v) of the root trochoid of an internal tooth are given by:

$$\begin{aligned} r(\varphi) &= \sqrt{\delta^2 + r_g^2 + 2\delta r_g \sin \varphi} \quad \text{for } \phi_g \leq \varphi \leq \frac{\pi}{2} \\ v(\varphi) &= \theta - \phi_g - \lambda \end{aligned} \quad \text{Equation 3.1}$$

where:

- r_g is the generating pitch radius of the internal tooth.
- ϕ_g is the generating pressure angle.
- δ is the distance from the generating pitch point to the generated trochoid point.
- θ, λ are the angles depicted in Figure A.2 in Annex A.
- φ is the parameter of the parametric polar equations and describes the point of the pinion-cutter fillet, which generates the corresponding point of the internal-tooth trochoid, as shown in

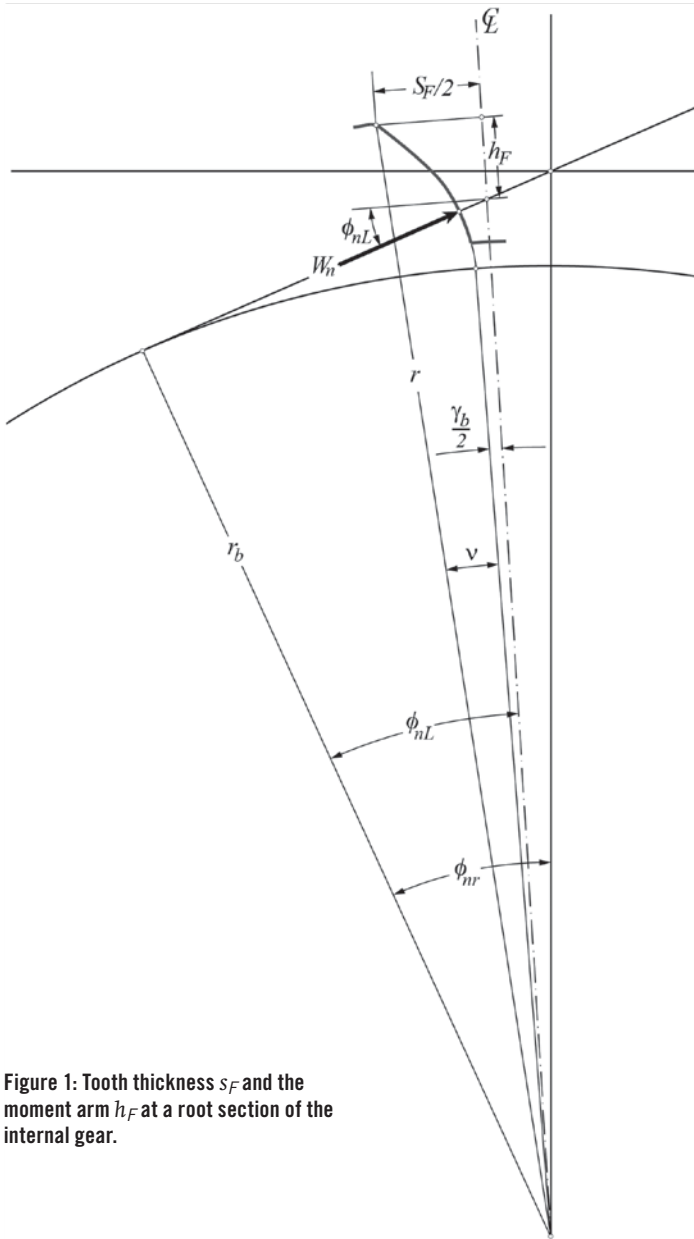


Figure 1: Tooth thickness s_F and the moment arm h_F at a root section of the internal gear.

Figure A.2 in Annex A.

The derivation of the equations for δ , θ , and λ are presented in Annex A. As seen in Figure 1, the tooth thickness s_F and the moment arm h_F at the root section described by φ are given by:

$$s_F(\varphi) = 2r(\varphi) \sin\left(v(\varphi) + \frac{\gamma_b}{2}\right) \quad \text{Equation 3.2}$$

$$h_F(\varphi) = r(\varphi) \cos\left(v(\varphi) + \frac{\gamma_b}{2}\right) - \frac{r_b}{\cos \phi_{nL}}$$

where:

γ_b is the angular thickness of the internal tooth involute at the base radius (which may be negative).

r_b is the base radius.

The base angular thickness and the load angle can be computed from:

$$\gamma_b = \frac{\pi}{N} + 4 \frac{x}{N} \tan \phi_n + 2(\tan \phi_n - \phi_n) \quad \text{Equation 3.3}$$

$$\phi_{nL} = \sqrt{\frac{r_L^2}{r_b^2} - 1} + \frac{\gamma_b}{2}$$

where:

- N is the number of teeth of the internal gear.
- x is the addendum modification coefficient on internal gear teeth.
- ϕ_n is the standard normal pressure angle.
- r_L is the radius of the HPSTC.

To locate the critical section with the Lewis parabola the value of the φ parameter providing the maximum value of the (h_F/s_F^2) should be found, for which an iterative procedure should be used, as the one presented in [5,7]. Probably, the simplest method to find the solution is the bisection method, which yields results almost instantaneously with modern high-speed computers.

Finally, the stress correction factor can be computed from [2]:

$$K_f = H + \left(\frac{s_F}{r_F}\right)^L \left(\frac{s_F}{h_F}\right)^M \quad \text{Equation 3.4}$$

where:

$$H = 0.331 - 0.436\phi_n$$

$$L = 0.324 - 0.492\phi_n$$

$$M = 0.261 + 0.545\phi_n$$

and:

r_F is the minimum curvature radius of the root fillet, which is computed as described in Annex B.

3.2 APPROACH #2, BASED ON AGMA 911-B21

For external and internal gears, AGMA 911-B21 [10] provides a calculation method of the J-factor based on the following assumptions:

- Both the bending component and the compressive component of the stress at the root should be considered.
- The root fillet is approximated to an arc of circumference.
- The stress correction factor is assessed at any section of the root.
- Stresses should be calculated at the tooth-root section in which the corrected stress is maximum, for the load acting at the HPSTC.

Accordingly, the stress correction factor is, in this case, expressed as:

$$K_f(\varphi) = H + \left(\frac{s_F(\varphi)}{r_F}\right)^L \left(\frac{s_F(\varphi)}{h_F(\varphi)}\right)^M \quad \text{Equation 3.5}$$

in which the correlation coefficients have been slightly modified, as follows:

$$H = 0.3255 - 0.4167\phi_n$$

$$L = 0.3318 - 0.5209\phi_n$$

$$M = 0.2682 + 0.5259\phi_n$$

To determine the critical section, the value of φ corresponding to the maximum of the function $\left[\kappa_f(\varphi) \left(\frac{h_F(\varphi)}{s_F(\varphi)} - \frac{\tan \phi_{nL}}{s_F(\varphi)}\right)\right]$ should be found. Once again, the simplest way to solve the problem is by using the bisection method. The derivation of the equations for the tooth thickness $s_F(\varphi)$ and the moment arm $h_F(\varphi)$ is presented in Annex C.

3.3 APPROACH #3, BASED ON HYBRID MODEL

The hybrid approach is similar to Approach #2 but considering the trochoidal root fillet. Consequently, the calculation of the J-factor is based on the following assumptions:

- Both the bending component and the compressive component of the stress at the root are considered.
- The stress correction factor is calculated considering the curvature radius of the trochoid at the corresponding point of the root fillet.
- Stresses should be calculated at the tooth-root section in which the corrected stress is maximum, for the load acting at the HPSTC.

Accordingly, the stress correction factor is, in this case, expressed as:

$$K_f(\varphi) = H + \left(\frac{s_F(\varphi)}{r_F(\varphi)}\right)^L \left(\frac{s_F(\varphi)}{h_F(\varphi)}\right)^M \quad \text{Equation 3.6}$$

in which the correlation coefficients have been taken as in Approach

#1. The critical section will be given by the value of φ corresponding to the maximum of the function $\left[K_f(\varphi) \left(\frac{h_{rF}(\varphi)}{s_F(\varphi)} - \frac{\tan \phi_{nl}}{s_F(\varphi)} \right) \right]$, which may be obtained from the bisection method. The equations for $s_F(\varphi)$, $h_{rF}(\varphi)$, and $r_F(\varphi)$ can be found in Annexes A and B.

4 FEA-BASED APPROACH

A FEA-based approach has been established to get reference values of the tooth root stresses and the corresponding J -factor and assess the effectiveness and accuracy of the analytical approaches proposed above. The 2D finite element model used in this work is shown in Figure 2. The FE model is generated automatically by a custom-made computer program considering the actual geometry of the gears, analyzed by a general-purpose finite element computer program, and the results automatically post-processed. The geometry of the internal gear will be generated by a shaper, so that the influence of the number of teeth of the shaper on the maximum bending stress will be studied as well.

The FE model of the gear set comprises three pairs of teeth. The finite element model of the internal gear considers 60 elements along the active profile, 30 elements along the fillet, and 10 elements along the top land. The number of elements of the upper rim sides depends on the number of elements of the top land, and the total number of elements on the bottom of the rim depends on the number of elements in the lower rim. For the external pinion, the model considers 50 elements along the active surface, 40 elements along the fillet, and 10 elements along the top land. To ensure the mesh density does not affect the resulting stresses, the number of elements in the fillet and active profile for both the external pinion and the internal gear was increased until any significant variation in maximum stresses became negligible.

To ensure consistent relative loads across various gear size configurations, an input torque of 10 N·m was initially applied to a reference case. This reference case consisted of a pinion with 25 teeth and an internal gear with 100 teeth, featuring a module of 1.0 mm and a pressure angle of 20 degrees. The face width is 10 mm. The fillet radius coefficient of the external pinion is 0.38, and the shaper tip radius coefficient is 0.25. The profile shift coefficients for both the external pinion and the internal gear are zero, and the center distance is always the standard. For the other different gear sets analyzed, the torque applied to the pinion was adjusted proportionally based on its pitch radius. This adjustment guarantees similar relative loads for all analyzed cases, even when the gear sizes vary considerably from one case to another.

All FE models will consider three pairs of teeth to have the rigid edges defined on both lateral sides of the rim far enough from the fillet on the driving side of the external pinion and driven side of the internal gear of the middle pair of teeth of the model (Figure 2). The torque is applied at the reference node of the pinion located on its axis of rotation. The bottom and lateral sides of the rim define rigid edges having their degrees of freedom related to those of the corresponding reference node. The reference node of the pinion is, constrained in all degrees of freedom except for rotation around the Z-axis, which is left unconstrained to receive the applied torque. For the internal gear, similar boundary conditions are established but, in this case, the reference node on the axis of rotation of the internal gear is constrained in all degrees of freedom, included the rotation in Z direction.

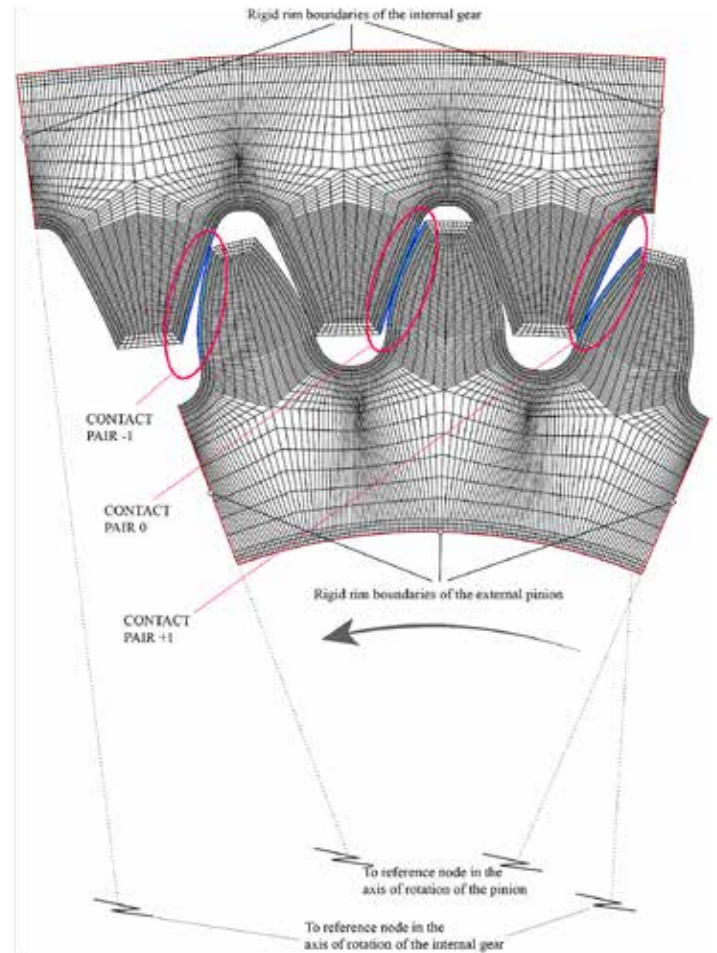


Figure 2: Finite element model of an internal spur gear set.

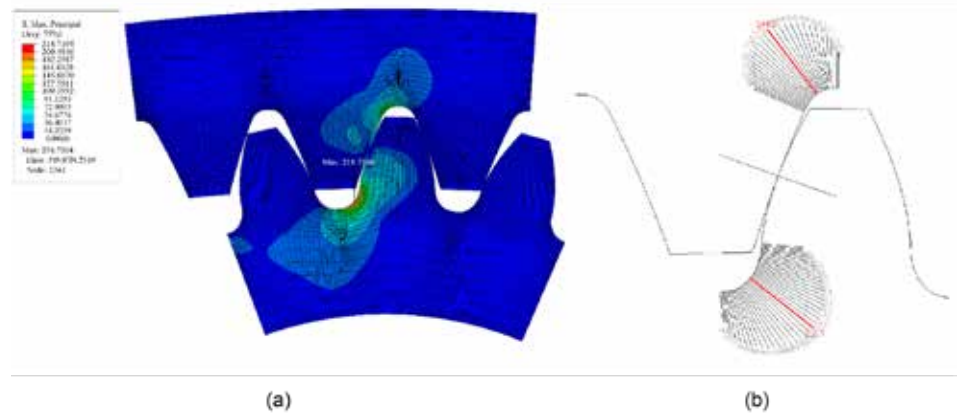


Figure 3: Results of FE analysis for the reference case with contact at the HPSTC of the pinion: (a) results from FE computer program; (b) results post-processed by a custom-made computer program.

Two different FE models will be used to get the J -factor based on the FEA results. The first model has only the middle contact pair 0 activated (see Figure 2), and the relative position of contact of the external pinion, and the internal gear is established at the HPSTC of the pinion teeth for the determination of the maximum stress at its tooth fillets, and similarly, it will be established at the HPSTC of the internal gear to get the maximum stress at its tooth fillets. Therefore, using this type of FE model, the load is supported by just one pair of teeth.

The second model considers not only the middle contact pair 0 activated, but it also considers the contact pair -1 on the previous pair of teeth and the contact pair +1 on the following pair of teeth activated

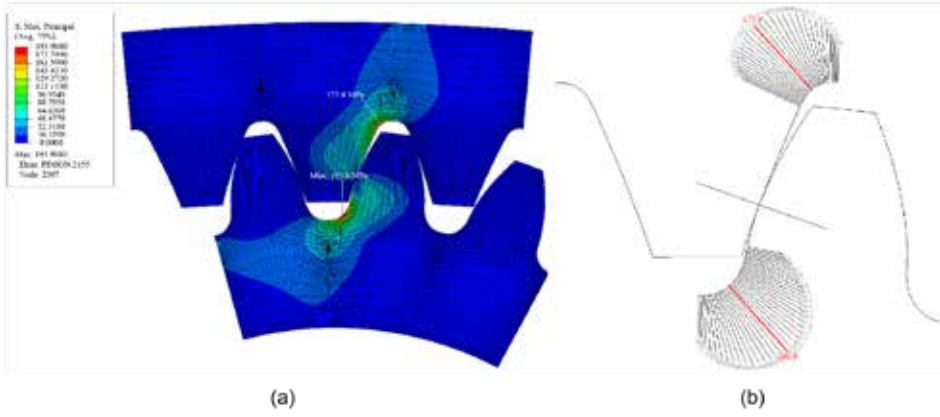


Figure 4: Results of FE analysis for the reference case with contact at the HPSTC of the internal gear: (a) results from FE computer program; (b) results post-processed by a custom-made computer program.

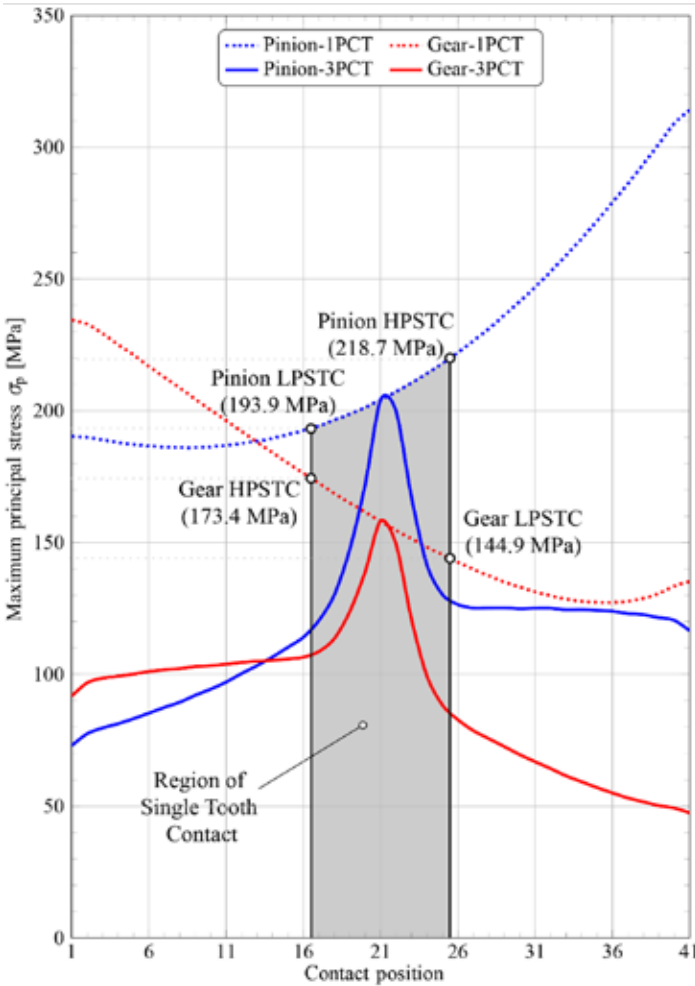


Figure 5: Maximum principal stress at the tooth fillet of the reference internal gear evaluated at 41 contact positions along the entire cycle of meshing of one tooth.

(see Figure 2). When using this model, an analysis along 41 contact positions has to be carried out to find the most unfavorable contact position yielding the maximum tooth root principal stress while considering the load shared between the different pairs of teeth in contact.

Tooth root stresses obtained from the FEA method for the external pinion, and the internal gear will be based on the maximum principal stress at the root fillet of the driving side of the external pinion and driven side of the internal gear.

Figure 3a shows the results of FE analysis for contact at the HPSTC of the pinion for the reference case mentioned above yielding a maximum principal stress of 218.7 MPa at the pinion root fillet. Figure 3b shows the results of the automatic post-processing of the results by the authors' custom-made computer program. Similarly, Figure 4a shows the results of FE analysis for the HPSTC of the internal gear yielding a maximum principal stress of 193.9 MPa, and Figure 4b shows the results of the authors' custom made-program. For both cases, the FE model only considers the middle contact pair, so there is no load shared between different pairs of contacting teeth.

Figure 5 presents the results of the FE analysis conducted for 41 contact positions

throughout the entire meshing cycle of a single tooth. The analysis spans from point 1, which represents the lower active contact point of the pinion in mesh with the tip point of the internal gear active profile, to point 41, which corresponds to the tip point of the pinion active profile in contact with the lower active contact point of the internal gear.

The stresses at the fillets of the external pinion and the internal gear for the contact positions shown in Figures 3 and 4 are also highlighted and shown in Figure 5 together with the results obtained for 41 contact positions throughout the entire meshing cycle of a single tooth. The region of single tooth contact is also shown as well as the result of FE analysis when the load is shared between different pairs of contacting teeth. In Figure 5, the label 1PCT stands for one pair of contacting teeth (no load shared) and the label 3PCT stands for three pairs of contacting teeth (load shared between different pairs of teeth). Due to the effect of the elastic deformation of the tooth due to bending and the elastic deformation at the area of contact, the effective contact ratio is increased and the load is transferred progressively between consecutive pairs of contacting teeth. For the reference case of design, as it can be observed in Figure 5, the effective contact ratio is very close to 2.0 because the region of single tooth contact is reduced to almost a single point near the pitch point.

Considering the maximum principal stress from FEA at the fillet nodes as σ_p , the corresponding J -factor will be evaluated by:

$$J = \frac{W_t}{Fm_n\sigma_p} \quad \text{Equation 4.1}$$

By applying Equation 4.1, the J -factor for the reference case of design along the 41 contact positions previously described is shown in Figure 6. The value of W_t is calculated at the operating pitch radius of the pinion or the gear, independently of the contact position being represented in the graph. The J -factor is inversely proportional to the maximum principal stress at the tooth fillet.

When using the FE model with the three contact pairs activated, the J -factor is evaluated as the minimum J -factor for all 41 contact positions along the entire cycle of meshing of one tooth as shown in Figure 6. When FE models with only the middle contact pair activated, the J -factor is evaluated at the pinion HPSTC and the wheel HPSTC as shown in Figure 6.

5 NUMERICAL RESULTS

AGMA 911-B21 [19] represents graphs of the J -factor for three different pressure angles: 20°, 22.5°, and 25°, for both the external gear in mesh with its internal gear mate, and for the internal gear in mesh with its external pinion mate. It is worth noticing the graphs shown in AGMA 911-B21 were obtained considering an addendum for the

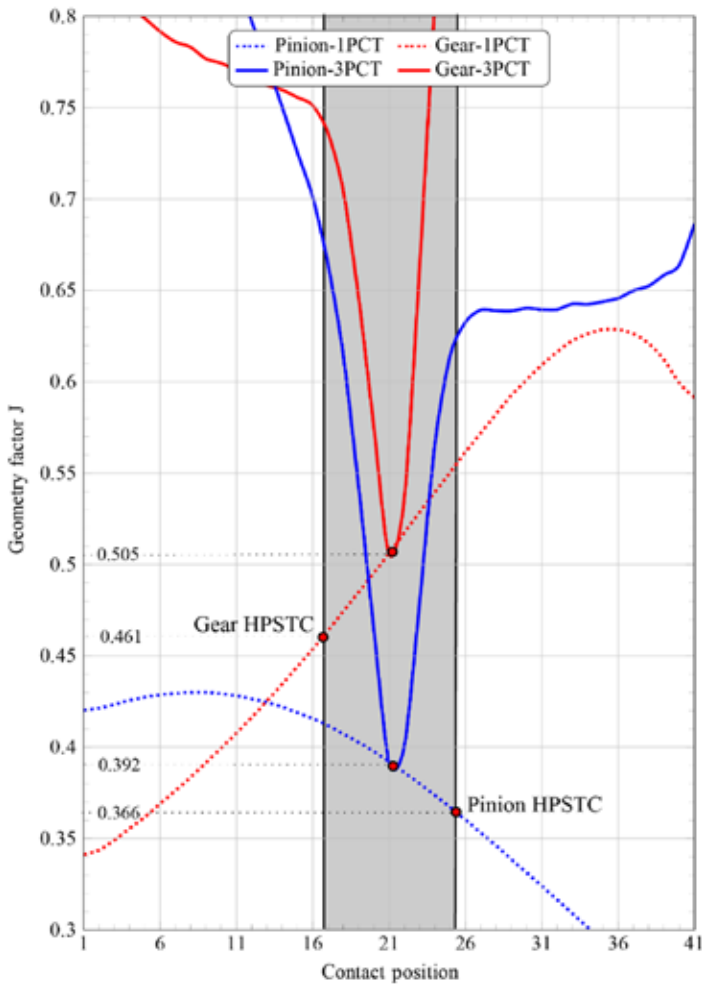


Figure 6: Geometry factor J for the reference internal gear set evaluated at 41 contact positions along the entire cycle of meshing of one tooth.

internal gear equal to 1.0. However, the addendum has to be shortened to avoid interference with the fillet of the pinion for some of the cases of design considered. Therefore, in this work, the addendum coefficient of the internal gear has been shortened and made equal to 0.8, whereas the addendum of the external gear is equal to 1.0. The dedendum coefficient for both the external pinion and the internal gears is considered equal to 1.25. For all cases of design, the pressure angle is 20° , and the module is 1.0 mm.

Figure 7 shows the geometry factor J for the external pinion (a) and the internal gear (b) according to the described approach #1. Similarly, Figures 8 and 9 show the geometry factor J for the external pinion (a) and the internal gear (b) according to the described Approaches #2 and #3, respectively. The same ranges of variation of the number of teeth of the external pinions and the number of teeth for the internal gears as considered in AGMA 911-B21 were considered here.

The J -factor for the external pinion or the internal gear shows similar tendencies for all three approaches. Approach #3 yields larger values of the J -factor in general for both the external pinion and the internal gear. This means the tooth-root stresses evaluated with Approach #3 will be lower than those evaluated with Approach #1. However, assessing which approach yields more accurate results is not yet possible as we lack baseline results to compare with. In order to overcome this issue, the finite element method is used to get reference values of the tooth root stresses and the results presented below.

5.1 FACTOR J EVALUATED BY FEA

Two FE models as described in Section 4 are applied here to evaluate

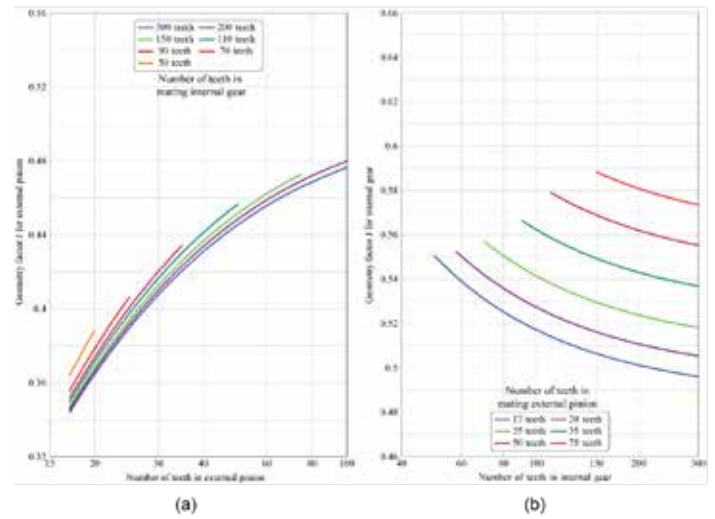


Figure 7: Geometry factor J evaluated according to Approach #1 for (a) external gears in mesh with their respective internal mates, and (b) internal gears in mesh with their respective external mates.

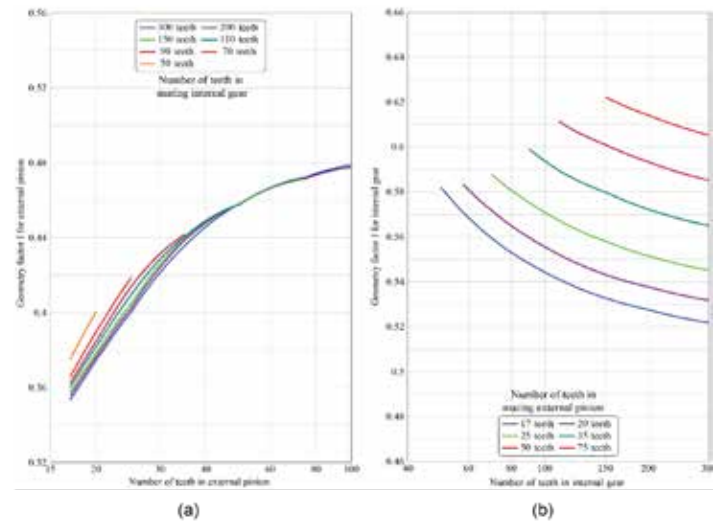


Figure 8: Geometry factor J evaluated according to Approach #2 for (a) external pinions in mesh with their respective internal mates, and (b) internal gears in mesh with their respective external mates.

the J -factor for the external pinion and the external gear by finite element analysis. The first model is based on the consideration of one pair of contacting teeth only, corresponding to the middle pair of teeth of the model and contact positions at the respective HPSTC of the external pinion and the internal gear. Figure 10a shows the J -factor for the external pinion is lower than the J -factor obtained with Approaches #1 to #3. For the internal gear, Figure 10b shows the J -factor is also lower than the J -factor obtained with Approaches #1 to #3. Therefore, if FEA models with full load applied at the HPSTC of the external pinion or the internal gear are used as baseline, the root stresses are underestimated by all analytical approaches.

Figure 11 shows the J -factor for the external pinion (Figure 11a) and the internal gear (Figure 11b) when FE models with three pairs of contacting teeth are used to evaluate the minimum J -factor along 41 contact positions covering the entire cycle of meshing of one tooth. Depending on the case evaluated, larger J -factors are obtained. The main reason for this is that, for internal spur gear sets, the effective contact ratio is in most of the cases larger than 2.0 and, therefore, the analytical approaches do not capture the load sharing between two or more pairs of contacting teeth.

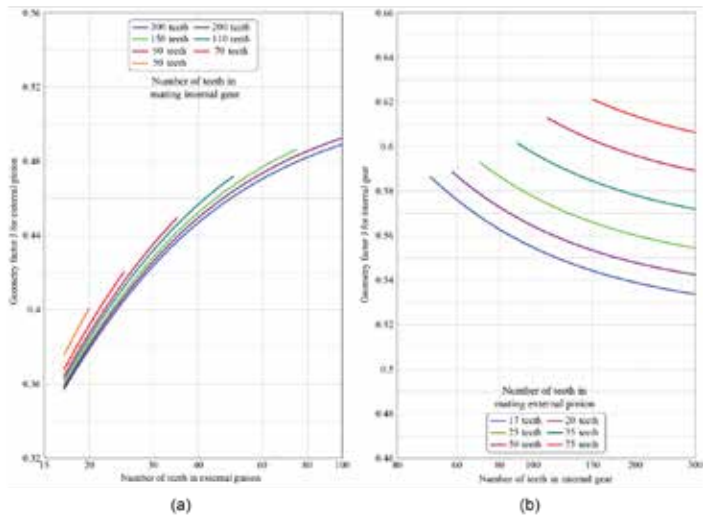


Figure 9: Geometry factor J calculated according to Approach #3 for (a) external gears in mesh with their respective internal mates, and (b) internal gears in mesh with their respective external mates.

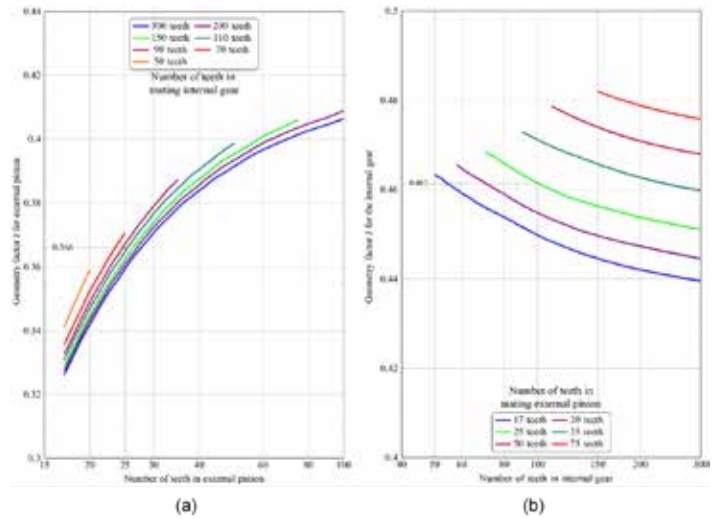


Figure 10: Geometry factor J for (a) external gears and (b) internal gears based on FEA and only one pair of contacting teeth with contact at their respective HPSTC.

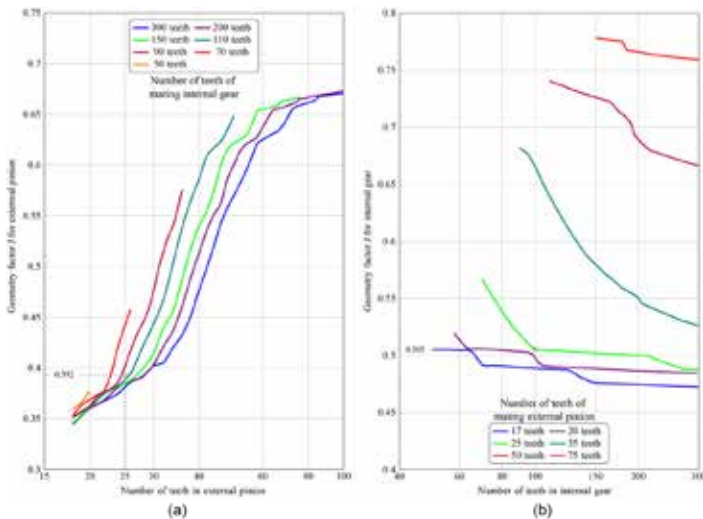


Figure 11: Geometry factor J for (a) external pinions and (b) internal gears based on FEA and load shared between different pairs of contacting teeth.

5.2 INFLUENCE OF THE NUMBER OF TEETH OF THE SHAPER

In order to investigate the influence of the number of teeth on the J -factor of internal gears, the actual trochoid profile of the internal gear generated by shapers with tooth numbers varying from 20 teeth to 100 teeth will be considered and the J -factor evaluated for seven different gear sets comprising an external pinion of 25 teeth in mesh with their respective internal mates having 50, 70, 90, 110, 150, 200, and 300 teeth. Figure 12a shows the J -factor for the internal gear of the seven gear sets evaluated using Approach #1 as a function of the number of teeth of the shaper that generates the internal gear. Figure 12b shows the J -factor evaluated based on FEA with one pair of contacting teeth and load applied at the HPSTC of the internal gear. The results indicate a decrease in the J -factor as the number of teeth on the generating shaper increases. The J -factor evaluated based on FEA further confirms this influence, demonstrating that the J -factor decreases as the number of teeth on the shaper increases.

6 CONCLUSIONS

The performed research allows the following conclusions to be drawn:

- Three analytical approaches to determine the J -factor for external pinions and internal gears considering different assumptions

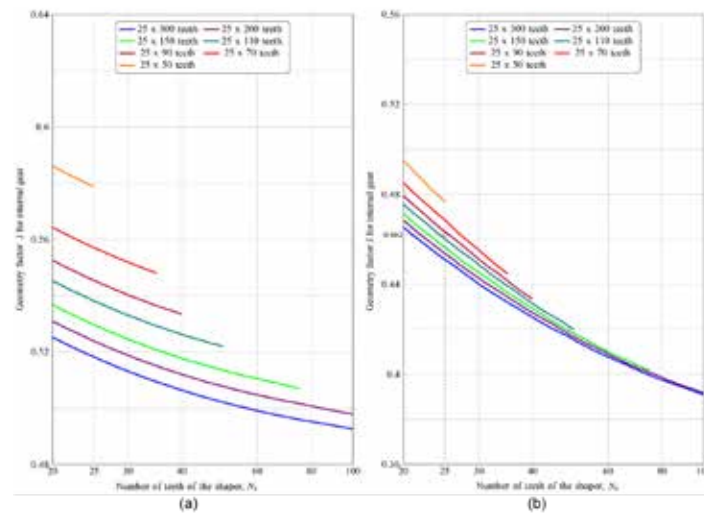


Figure 12: Geometry factor J for internal gears with pressure angle 20° in mesh with their respective 25-teeth external pinions as a function of the number of teeth of the shaper: (a) J -factor based on application of Approach #1; (b) J -factor based on FEA with only one pair of contacting teeth and load applied at the HPSTC of the internal gear.

about the geometry of the trochoid, localization of the critical tooth section and curvature radius to be considered for the evaluation of the stress concentration factor has been evaluated and compared. All three methods show similar tendencies with respect to the variation of the number of teeth, with Approach #3 yielding the larger values of the J -factor and therefore the less conservative values of the tooth root stress.

► The number of teeth on the shaper has a significant influence on the J -factor for internal gears, which is not adequately accounted for in Approach #2, based on the method described in the Information Sheet AGMA 911-B21, Annex A. Therefore, it is recommended to consider the number of teeth of the shaper when formulating any future proposal aimed at developing a more precise procedure for determining the J -factor in internal spur gears.

The J -factor based on the FEA approach shows similar tendencies but large differences with respect to the J -factor based on analytical approaches. The main reason is the effective contact ratio might be larger than 2.0 for most cases of design of internal gears and, therefore, any current analytical approach to determine the J -factor does

not take it into account. Also, the stress concentration factor usually applied for external gears might not be applicable for internal gears. A comprehensive study based on finite element analysis should be carried out to evaluate the stress concentration factor in internal gears. Future procedures to determine the J -factor in internal spur gears should be considering the determination of the effective contact ratio based on the applied load as well as considering an updated stress concentration factor.

7 ACKNOWLEDGEMENTS

The authors express their deep gratitude to the Spanish Council for Scientific and Technological Research for the support of the project PID2019-110996RB-I00 "Simulation and control of transmission error of cylindric gears," as well as the School of Engineering of UNED for the support of the action 2023-ETSII- UNED-04, "Optimization of transmission error in spur gears with profile modification."

ANNEX A: GENERATION OF THE TROCHOID OF INTERNAL TEETH

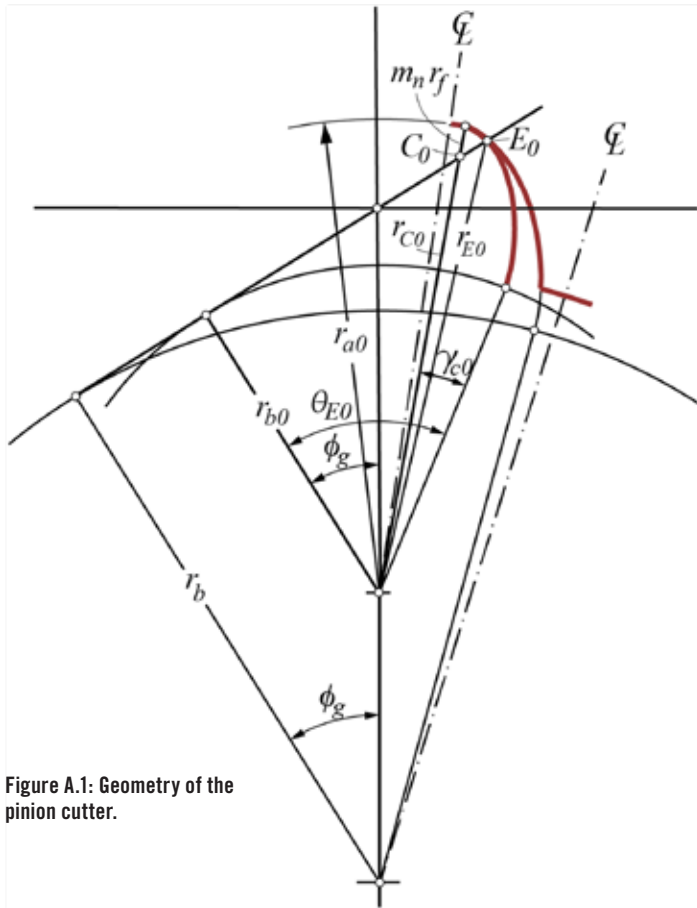


Figure A.1: Geometry of the pinion cutter.

GEOMETRY OF THE PINION CUTTER

The pinion cutter will be described with subscript 0. From Figure A.1, the radius of the center of the tip fillet is:

$$r_{c0} = r_{a0} - m_n r_f \quad \text{Equation A.1}$$

where:

r_{a0} is the addendum radius of the pinion cutter.

r_f is the tool tip radius coefficient.

The radius of the inner point of the cutter fillet, which is tangent to the cutter involute, is:

$$r_{E0} = \sqrt{r_{b0}^2 + \left(m r_f + \sqrt{r_{c0}^2 - r_{b0}^2} \right)^2} \quad \text{Equation A.2}$$

and the angles θ_{E0} and ν_{C0} are:

$$\theta_{E0} = \frac{1}{r_{b0}} \left(m r_f + \sqrt{r_{c0}^2 - r_{b0}^2} \right) \quad \text{Equation A.3}$$

$$\nu_{C0} = \theta_{E0} - \cos^{-1} \frac{r_{b0}}{r_{c0}}$$

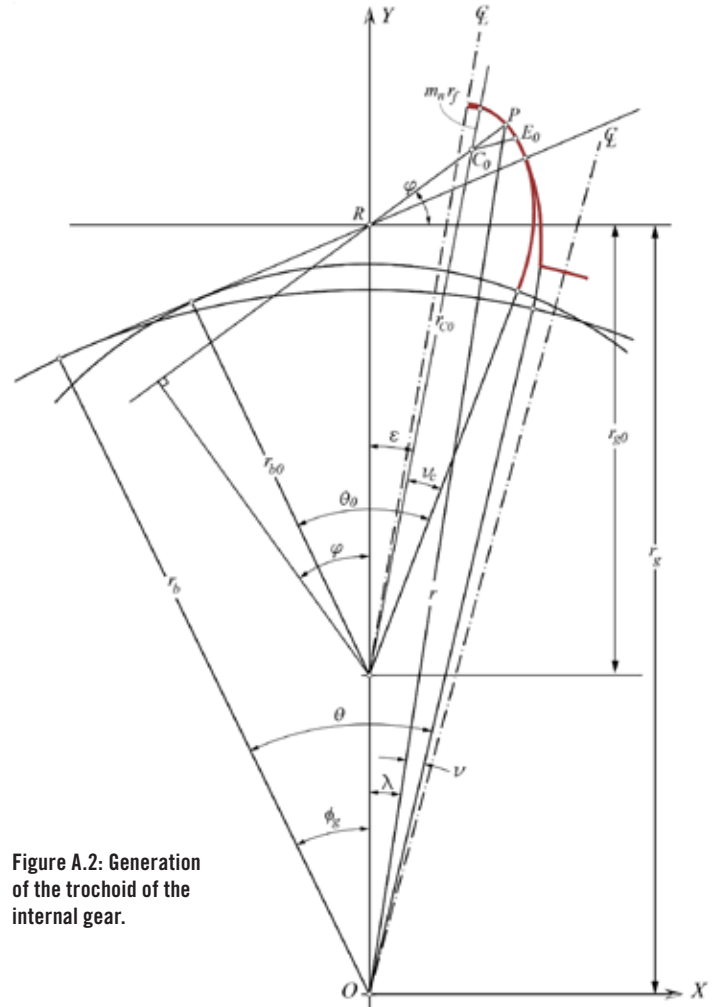


Figure A.2: Generation of the trochoid of the internal gear.

EQUATION OF THE ROOT FILLET

Figure A.2 depicts the relative position of the pinion cutter and the generated internal gear in which the cutter fillet point described by φ is generating the point P at the root fillet of the internal tooth. From this figure, the distance between point P and the pitch point R is:

$$\delta(\varphi) = \sqrt{r_{c0}^2 - r_{g0}^2 \cos^2 \varphi - r_{g0} \sin \varphi + m r_f} \quad \text{Equation A.4}$$

where:

r_{g0} is the generating pitch radius of the cutter, which is given by:

$$r_{g0} = \frac{r_{b0}}{\cos \phi_g} \quad \text{Equation A.5}$$

where:

ϕ_g is the generating pressure angle, which can be computed by solving the equation:

$$\left(\tan \phi_g - \phi_g \right) = \left(\tan \phi_n - \phi_n \right) + 2 \frac{x - x_0}{N - N_0} \quad \text{Equation A.6}$$

From Figure A.2, the radius of the generated point of the internal tooth root trochoid is:

$$r^2(\varphi) = \delta^2(\varphi) + r_g^2 - 2\delta r_g \cos \left(\varphi + \frac{\pi}{2} \right) \quad \text{Equation A.7}$$

$$r(\varphi) = \sqrt{\delta^2(\varphi) + r_g^2 + 2\delta r_g \sin \varphi}$$

and, from the same figure, the polar angle is:

$$v(\varphi) = \theta - \phi_g - \lambda$$

Angles λ and θ can be computed from:

$$\lambda(\varphi) = \sin^{-1} \left(\frac{\delta(\varphi)}{r(\varphi)} \cos \varphi \right)$$

$$\theta(\varphi) = \frac{r_b - r_{b0}}{r_b} \tan \phi_g + \frac{r_{b0}}{r_b} \theta_0(\varphi)$$

in which $\theta_0(\varphi)$ is:

$$\theta_0(\varphi) = v_{c0} + \varepsilon(\varphi) + \phi_g$$

$$\varepsilon(\varphi) = \sin^{-1} \left(\frac{\delta - m_n r_f}{r_{c0}} \cos \varphi \right)$$

Summarizing, according to Equations a.7 and a.8, the equation of the generated root fillet is:

$$r(\varphi) = \sqrt{\delta^2 + r_g^2 + 2\delta r_g \sin \varphi} \quad \text{for} \quad \phi_g \leq \varphi \leq \frac{\pi}{2}$$

$$v(\varphi) = \theta - \phi_g - \lambda$$

ANNEX B: CURVATURE RADIUS OF THE GENERATED ROOT FILLET

From Figure A.2, the normal line to the generated trochoid through the point P is placed over the segment RP. The equation of this normal line respect to the reference system (O, X, Y) represented in Figure A.2 is:

$$[r(\varphi)] = \begin{bmatrix} s \cos \varphi \\ r_g + s \sin \varphi \end{bmatrix}$$

After a small rotation $d\alpha$ of the gear during the generation, the above line moves and reaches the position described by the equation:

$$[r(\varphi)]_{d\alpha} = \begin{bmatrix} \cos d\alpha & \sin d\alpha \\ -\sin d\alpha & \cos d\alpha \end{bmatrix} \begin{bmatrix} s \cos \varphi \\ r_g + s \sin \varphi \end{bmatrix} = \begin{bmatrix} r_g d\alpha + s(\cos \varphi + \sin \varphi d\alpha) \\ r_g + s(\sin \varphi - \cos \varphi d\alpha) \end{bmatrix}$$

Equation A.8

Equation A.9

Equation A.10

Equation A.11

Equation B.1

Equation B.2

At this position, a new fillet point is generated, and its normal line can be expressed as:

$$[r(\varphi + d\varphi)] = \begin{bmatrix} t \cos(\varphi + d\varphi) \\ r_g + t \sin(\varphi + d\varphi) \end{bmatrix} = \begin{bmatrix} t(\cos \varphi - \sin \varphi d\varphi) \\ r_g + t(\sin \varphi + \cos \varphi d\varphi) \end{bmatrix}$$

The center of curvature will be defined by the intersection of two normal lines. Equalizing the Y-coordinates of Equations b.2 and b.3, it is obtained:

$$t = \frac{\sin \varphi - \cos \varphi d\alpha}{\sin \varphi + \cos \varphi d\varphi} s$$

and equalizing the X-coordinates, it is obtained:

$$s = -r_g(\sin \varphi + \cos \varphi d\varphi) \frac{d\alpha}{d\alpha + d\varphi}$$

$$t = -r_g(\sin \varphi - \cos \varphi d\alpha) \frac{d\alpha}{d\alpha + d\varphi}$$

and neglecting infinitesimals of higher order:

$$s = t = -r_g \sin \varphi \frac{d\alpha}{d\alpha + d\varphi}$$

From Figure A.2, the rotation $d\alpha$ of the generated gear corresponds to a rotation $d\varepsilon$ of the pinion cutter, and therefore:

$$\frac{d\alpha}{d\varphi} = \frac{N_0}{N} \left(\frac{d\varepsilon}{d\varphi} \right)$$

If, for simplicity, $d\alpha/d\varphi$ is denoted by K , from Equation a.10 it is obtained:

$$K(\varphi) = \frac{\frac{N_0}{N}}{\sqrt{r_{c0}^2 - (\delta(\varphi) - m_n r_f)^2 \cos^2 \varphi}} \left(\frac{r_{g0}^2 \cos^2 \varphi \sin \varphi}{\sqrt{r_{c0}^2 - r_{g0}^2 \cos^2 \varphi}} - r_{g0} \cos^2 \varphi - (\delta(\varphi) - m_n r_f) \sin \varphi \right)$$

and Equation b.6 results in:

$$s = -r_g \sin \varphi \frac{K(\varphi)}{K(\varphi) + 1}$$

The coordinates of the center of curvature can be obtained by replacing Equation b.9 in Equation b.2:



$$X_{CC}(\varphi) = -r_g \frac{K(\varphi)}{K(\varphi) + 1} \sin \varphi \cos \varphi \quad \text{Equation B.10}$$

$$Y_{CC}(\varphi) = r_g - r_g \frac{K(\varphi)}{K(\varphi) + 1} \sin^2 \varphi$$

The curvature radius is the distance from the center of curvature to the generated point P, whose coordinates are:

$$\begin{aligned} X_P(\varphi) &= \delta(\varphi) \cos \varphi \\ Y_P(\varphi) &= r_g + \delta(\varphi) \sin \varphi \end{aligned} \quad \text{Equation B.11}$$

Consequently, the curvature radius at any point of the root fillet is given by:

$$r_F(\varphi) = \delta(\varphi) + r_g \frac{K(\varphi)}{K(\varphi) + 1} \sin \varphi \quad \text{Equation B.12}$$

The minimum radius of curvature T_{Fmin} , to be considered for the stress correction factor according to Dolan and Broghamer [2], corresponds to $\varphi = \eta/2$.

ANNEX C. EQUATIONS OF THE CIRCULAR ROOT FILLET

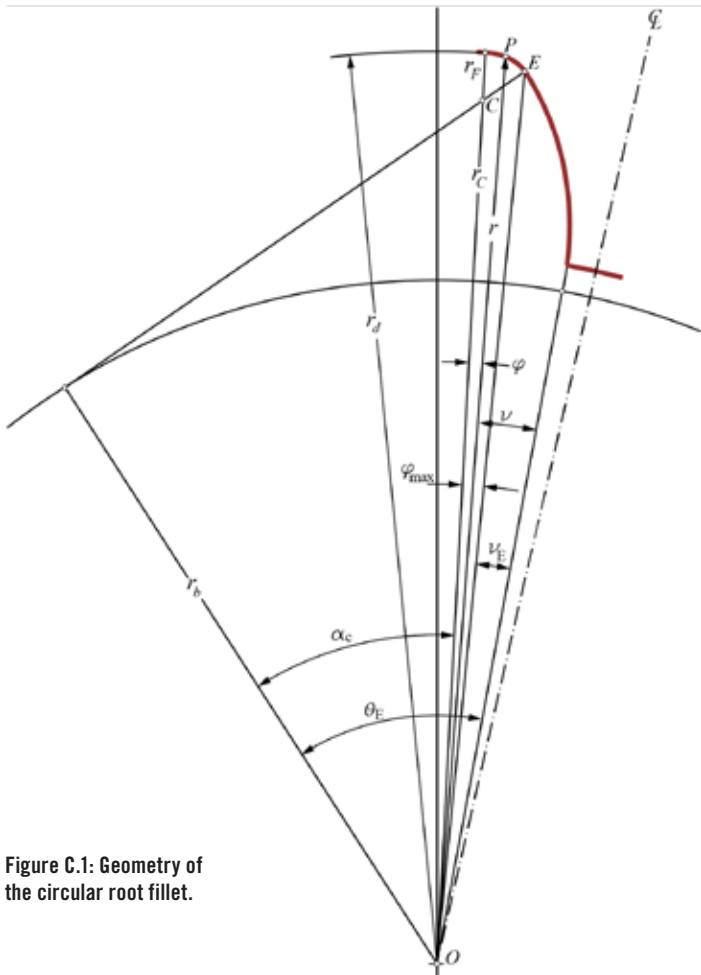


Figure C.1: Geometry of the circular root fillet.

From Figure C.1, the radius of the center of the root fillet is:

$$r_C = r_d - r_F \quad \text{Equation C.1}$$

where:

r_d is the dedendum radius of the internal gear.

Angles θ_E , ν_E , and α_C are given by:

$$\begin{aligned} \theta_E &= r_F + \sqrt{r_C^2 - r_b^2} \\ \nu_E &= \theta_E - \tan^{-1} \theta_E \\ \alpha_C &= \cos^{-1} \frac{r_b}{r_C} \end{aligned} \quad \text{Equation C.2}$$

consequently, the angle φ_{max} in Figure C.1 is:

$$\varphi_{max} = \theta_E - \nu_E - \alpha_C = \tan^{-1} \theta_E - \alpha_C \quad \text{Equation C.3}$$

The polar coordinates of the point P of the root fillet corresponding to the angle φ depicted in Figure C.1 can be calculated from the triangle OCP, as follows:

$$\begin{aligned} r(\varphi) &= \sqrt{r_C^2 + r_F^2 + 2r_C r_F \cos(\varphi + \varphi')} \\ \nu(\varphi) &= \nu_E + \varphi_{max} - \varphi \end{aligned} \quad \text{Equation C.4}$$

where:

$$\varphi' = \sin^{-1} \left(\frac{r_C}{r_F} \sin \varphi \right) \quad \text{Equation C.5}$$

BIBLIOGRAPHY

- [1] Lewis, W., 1893, "Investigation of the Strength of Gear Teeth," Proc. of the Engineers Club, 16-23, Philadelphia, PA.
- [2] Dolan, T.J. and Broghamer, E.L., 1942, "A Photoelastic Study of the Stresses in Gear Tooth Fillets," University of Illinois, Engineering Experiment Station Bulletin No. 335, Urbana, IL.
- [3] Errichello, R., 1983, "An Efficient Algorithm for Obtaining the Gear Strength Geometry Factor for Shaper Cut Gears," AGMA Paper P 139.05.
- [4] AGMA Information Sheet 908-B89, 1989, "Geometry Factors for Determining the Pitting Resistance and Bending Strength of Spur, Helical and Herringbone Gear Teeth," American Gear Manufacturers Association, Alexandria, VA.
- [5] Mitchiner, R.G. and Mabie, H.H., 1980, "The Determination of the Lewis Form Factor and the AGMA Geometry Factor J for External Spur Gear Teeth," Journal of Mechanical Design, 104(1): 148-158.
- [6] Carroll, R.K. and Johnson, G.E., 1988, "Approximate Equations for the AGMA J-Factor," Mechanism and Machine Theory, 23(6): 449-450.
- [7] Pedrero, J.I., Fuentes, A. and Estrems, M., 2000, "Approximate Method for the Determination of the Bending Strength Geometry Factor for External Spur and Helical Gear Teeth," Journal of Mechanical Design, 122(3): 331-336.
- [8] Arıkan, M.A.S., 2001, "Derivation of Analytical Expressions for Calculation of AGMA Geometry Factor J for External Spur Gears," Proc. ASME 2001 International Design Engineering Technical Conferences and Computers and Information in Engineering Conference, Volume 2B, 1033-1042, Pittsburgh, PA.
- [9] Arıkan, M.A.S., 2002, "Direct Calculation of AGMA Geometry Factor J by Making use of Polynomial Equations," Mechanics Research Communications, 29(4): 257-268.
- [10] AGMA Information Sheet 911-B21, 2021, "Design Guidelines for Aerospace Gear Systems," American Gear Manufacturers Association, Alexandria, VA.
- [11] AGMA Standard 2001-D04, 2004, "Fundamental Rating Factors and Calculation Methods for Involute Spur and Helical Gear Teeth," American Gear Manufacturers Association, Alexandria, VA.